DOI: 10.1002/cphc.200900734

Construction and Photophysical Properties of Organic–Inorganic Nanonetworks Based on Oligo(phenylenevinylene) and Functionalized Gold Nanoparticles

Jien Yang, Xiaofeng Liu, Changshui Huang, Chunjie Zhou, Yuliang Li,* and Daoben Zhu[a]

Novel organic–inorganic nanonetworks of oligo(phenylenevinylene) (OPV) and gold nanoparticles (GNPs) have been synthesized by the amine-based epoxide ring-opening reaction. The resulting OPV–GNPs nanocomposites exhibit homogeneous and well-defined interfaces between the organic ligands and the inorganic nanoparticles, thereby promoting efficient electronic interfacial interaction between the two constituents. The functionalized gold nanoparticles serve as chemical reagents for the construction of nanohybrids, while the epoxide-terminated OPV acts as linkage between gold nanoparticles. The new architecture provides a facile methodology for fabrication of novel organic–inorganic nanohybrids under relatively mild conditions, which facilitates further applications of hybrid materials.

1. Introduction

The design and fabrication of organic/inorganic nanostructures have been investigated intensively in the past decades owing to their significant promise in the area of catalysis,[1] photography,[2] optoelectronics,[3] surface enhanced Raman scattering (SERS),[4–5] and biomedical applications.[2,6–16] Metal nanoparticles exhibit intense size- and shape-dependent properties due to the surface plasmon resonance (SPR).[15–17] Therefore, they are an increasing important colorimetric reporter[18–19] for indicating the status of metal nanoparticles transferring from dispersion to aggregation.[4] Significant achievements have been made in synthesis of diverse functionalized gold nanoparticles (GNPs), referencing as monolayer protected gold clusters (MPCs).[20–21] which are usually exploited as building blocks for supramolecular structures and sensory applications.[22–26] The construction of such composite materials on the nanoscale is of great importantance in driving the development of nanotechnology. An appropriate architecture is appreciated for efficient dispersion of metal nanoparticles in organic media with well-defined interfaces and properties, in which the organic ligands effectively prevent metal nanoparticles from aggregation.[27]

Hybrid nanomaterials of GNPs and organic ligands are receiving considerable attention.[22–23] The organic ligands play an important part in fabrication of such systems, which include low molecular weight ligands[28–30] and polymers (both conjugated[31–32] and nonconjugated).[33–34] Oligo(phenylenevinylene) (OPV) and its derivatives are excellent candidates in linking the inorganic functional centers owning to their remarkable optical and electronic properties.[35] Thus, the combination of GNPs and OPV may bring out unique materials holding novel chemical and physical properties that can be exploited for fabrication of novel nanoscale devices.

Developing a methodology capable of efficiently and reproducibly fabricating molecular structure on atomic and macroscopic dimensions is a key factor in designing materials with pre-programmed activity, which remains a primary challenge in nanotechnology. Current trends for preparation of hybrid materials mainly include mixing these two components or constructing them either physically or chemically. The defect is the readily separation of the components and suppressing electronic interaction. This implies that the OPV–GNPs network with homogeneous phases and well-controlled interfaces are favorable for electronic communication and charge transportation, which is difficult to achieve just by utilizing conventional blending approaches.[36–37]

The nucleophilic opening of epoxide rings by amines (Scheme 1) is an important reaction for synthesis of polymers[38] and pharmaceuticals[39], which can be expedited effectively with zinc(II) perchlorate hexahydrate as a catalyst under relatively mild conductions. Herein, we present a facile pathway for fabrication of GNPs–OPV nanohybrids by utilizing an oligo(phenylene vinylene) tailored with epoxide groups, which acts as a linkage during the construction of nanohybrids with amino-functionalized GNPs. The as-prepared hybrid nanonetworks display homogeneous status and well-defined interfaces,

[a] J. Yang, Dr. X. Liu, Dr. C. Huang, C. Zhou, Prof. Y. Li, Prof. D. Zhu
Beijing National Laboratory for Molecular Sciences (BNLMS)
CAS laboratory of Organic Solids, Institute of Chemistry
Chinese Academy of Sciences and
Graduate School of Chinese Academy of Sciences
Beijing 100190 (Peoples Republic of China)
Fax: (+86) 10-82616576
E-mail: ylli@iccas.ac.cn

Supporting information for this article is available on the WWW under http://dx.doi.org/10.1002/cphc.200900734.

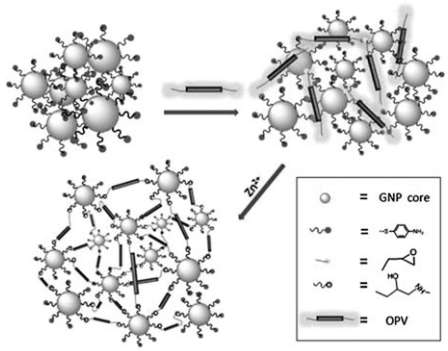

Scheme 1. Schematic illustration for the GNPs–OPV nanonetworks based on the epoxide ring-opening reaction.

which facilitate the electronic interaction between GNPs and OPV. Moreover, both the photophysical properties and morphology are dramatically influenced, indicating the validity of the combination between the two components.

2. Results and Discussion

2.1. Synthesis of Oligo(phenylenevinylene)

We adopted the Wittig–Horner reaction for olefin formation as reported[31] to synthesize the oligo (phenylenevinylene) as shown in Scheme 2. The bis-phosphonate 4[40] and 4-(oxiran-2-ylmethoxy) benzaldehyde **1** were reacted in dry DMF in the presence of excess amount of NaH to afford OPV ligand **5**.

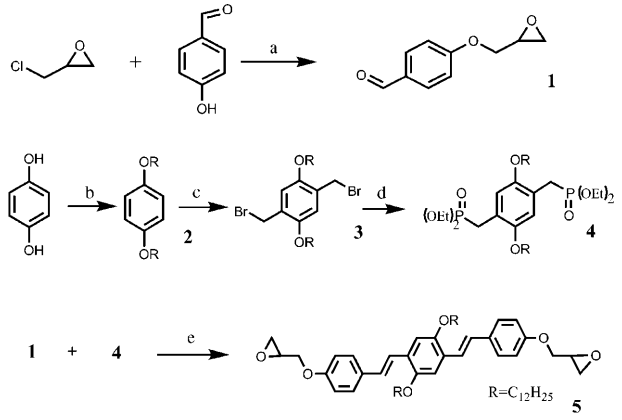

Scheme 2. Synthesis of OPV. Conditions for reactions: a) K_2CO_3, DMF; b) KOH, EtOH,$C_{12}H_{25}Br$; c) HBr(aq.), acetic acid; d) $P(OEt)_3$; e) NaH, THF.

2.2. Synthesis of Amino-Functionalized Gold Nanoparticles

The GNPs were synthesized utilizing the modified Brust's reaction[41] followed by ligand place-exchange reaction of tetra-n-octylammonium bromide (TOAB)-protected GNPs with 4-ATP.[42] In the ligand place-exchange reaction, a new thiolate ligand (4-ATP) was incorporated into nanoparticles by mixing the new ligand and the TOAB-protected GNPs in THF. The amino-functionalized gold nanoparticles were obtained as the final product after general workup.

The oligo (phenylenevinylene) was synthesized using the Wittig–Horner reaction.[40] The absorption maximum of OPV is located at 396 nm (Figure 1 A), which is mainly due to π–π^*

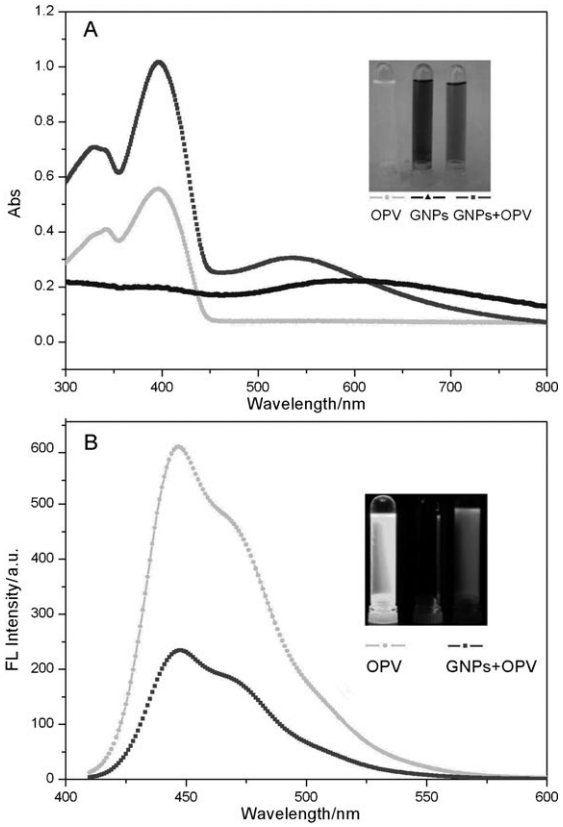

Figure 1. Spectrum of GNPs, GNPs–OPV, and OPV. A) the absorption spectra of GNPs GNPs–OPV, and OPV. Inset pictures are the OPV, GNPs and GNPs–OPV photographs. B) the emission spectra of GNPs–OPV and OPV. Inset pictures are the fluorescence of OPV, GNPs and GNPs–OPV.

transition of the conjugated main chains. The as-prepared OPV also acted as a fluorescent probe for indicating the reaction of amino-functionalized GNPs with epoxide beyond the role of linkage. The amino-functionalized GNPs were synthesized following a modified literature method, the TOAB protected GNPs underwent a ligand-exchange process by mixing the GNPs with quantitative amount of 4-ATP. The amino-functionalized GNPs are particularly prone to sedimentation within one minute[43] in most solvents. Therefore the GNPs could not be characterized by NMR due to poor solubility. So we demonstrated the reliability of the reaction using a model reaction (see Supporting Information). The sample was further inspected by transmission electron microscopy (TEM) and dynamic light scattering (DLS).

The SPR band of GNPs locates at 605 nm, giving a light blue coloration in transmission, which tends to suggest a distribution in the degree of aggregation in solution. The aggregation of amino-terminated GNPs is attributed to H-bonding between nanoparticles, leading to the formation of irregular fractal type

structures (Figure 5 A). The existence of SPR demonstrates the average diameter of GNPs larger than 5 nm, which also be confirmed by calculation from TEM observations. The DLS also give an evidence of the aggregation (the average diameter of GNPs larger than that of calculation from TEM) and the relatively narrow distribution of GNPs.

2.3. Construction of the Nanonetworks of OPV and GNPs

The organic–inorganic nanonetworks are usually fabricated using a common two-stage approach.[44] In the present study, we also take two steps for preparation of the nanohybrid. We have firstly prepared an epoxide-bearing OPV containing double epoxide at its junction point (Scheme 2). In a separate synthesis, we prepared amino-functionalized GNPs. Then, the GNPs was covalently linked on the OPV under relatively mild conditions in the presence of zinc perchlorate hexahydrate as catalyst.[39] The strategy avoids sacrificing the stability and photophysical properties of the two components.[45] Briefly, the solution of OPV (1×10^{-3} M) was mixed with an amount of amino-GNPs in DMF. And the mixture was left to react at ambient conditions with the presence of zinc perchlorate hexahydrate, while the changes were monitored over time using TLC. The quenching of fluorescence (Figure 1 B) of the OPV shows the progressive reaction procedure between the both components, demonstrating the GNPs disturb the electron transition of the conjugated main chains.

Fourier transform infrared spectroscopy (FT–IR) is a powerful tool to investigate the structures of molecules, which can identify certain functional groups. We explored the FT–IR of the 4-ATP, GNPs, OPV and the GNPs–OPV nanonetworks respectively. The IR spectra (Figure 2) shows the changes of critical functional groups before and after the reaction, verifying the combination of OPV and GNPs. From comparison the spectrum of 4-ATP and GNPs, the lack of S–H band at 3435 cm^{-1} support the formation of S–Au bond between the ligand of 4-ATP and the nanoparticles, while the presence of the N–H bond stretching signal occurs at 3380 cm^{-1}. This illustrates the structure detail of the 4-ATP protected GNPs. As a consequent of the ring-opening reaction of the amine attaching to the epoxide, the hydroxyl group emerges after the reaction. The presence of hydroxyl stretching modes at 3500 cm^{-1} is unambiguous evidence of the amino attaching to the epoxide.

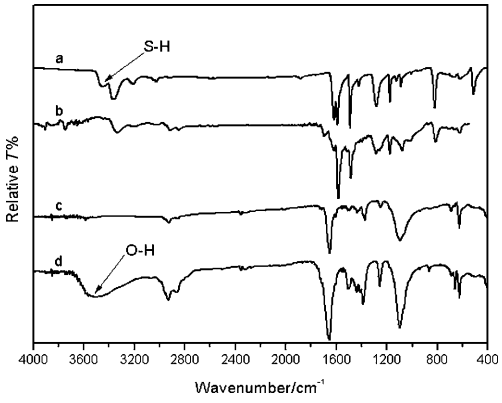

Figure 2. FT–IR spectra of a) 4-ATP, b) GNPs, c) OPV and d) GNPs–OPV. The samples were prepared by evaporating the solvent of the corresponding solutions on NaBr disks.

In the nanonetworks, the OPV acts as electron donor as well as a linkage, while the amino-GNPs acts as electron acceptor with amine attaching on the end of OPV. Unfortunately, the formed GNPs–OPV nanohybrid cannot be directly characterized by NMR spectroscopy because of its poor solubility. The UV/Vis absorption spectroscopy and TEM provide more direct insights for the reaction inducing the covalent combination of the two components. In Figure 1 the surface plasmon resonance peak of GNPs in the nanonetworks shifts from 605 nm to 538 nm owning to the improvement of GNPs dispersity within the system. The OPV acts as a spacer to prevent the GNPs from aggregation, which is the main function in the construction of the nanocomposites with wonderful interfaces. The formation of hydroxyl also suppress H-bonding between nanoparticles. The emission spectrum (Figure 1 B) indicates that the fluorescence of OPV is quenched, which also indicates that the GNPs are attached to the OPV effectively. The electronic transmission from OPV to GNPs upon the irradiation of light brings about the phenomenon.

The results of DLS confirm the topography of the GNPs and OPV–GNPs we draw from the TEM. From the histogram of Figure 3 A, we can understand the poor distribution of 4-ATP protected GNPs readily. The H-bonding forming between the nanoparticle results in a minor aggregation network. The networks' average diameter is larger than that of OPV–GNPs, which also is a proof of the conformation of nanonetworks. We have examined the effect of the molar ratio (*r*) between GNPs and OPV. As shown in Figure 4 A, the blue shift demonstrates the role of OPV in constructing the nanonetworks as the molar ratio decreases and the SPR and fluorescence increases. There is a saturation ratio between the GNPs and OPV, which most likely results from the space limits.

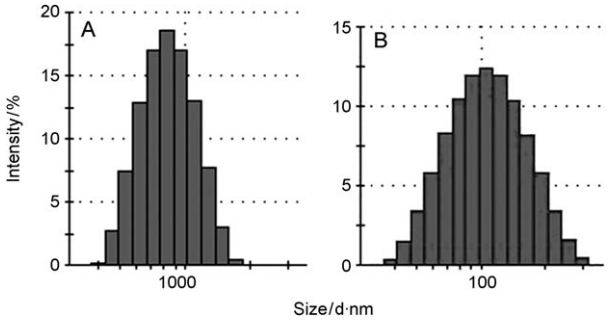

Figure 3. The size distribution of GNPs and OPV–GNPs nanonetworks: A) The diameter distribution of GNPs; B) The diameter distribution of OPV–GNPs.

From the TEM images in Figure 5, we notice the distinct changes happening between nanoparticles through the reaction. The image of Figure 5 A displays the aggregation of GNPs, which mainly can be contributed to the H-bonding inter-nanoparticles. The amino groups stretch out of the surfaces of

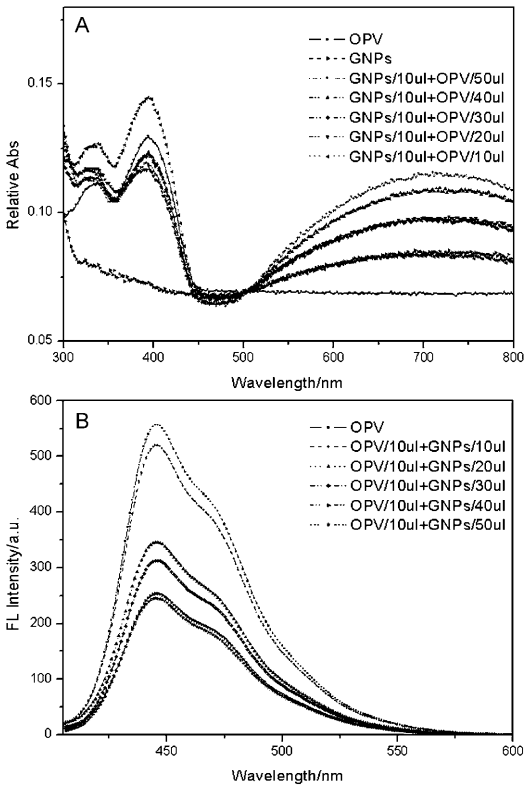

Figure 4. Spectra of different molar ratio between the OPV and GNPs. A) Absorption spectra. B) Emission spectra. The spectra were obtained from the solution of DMF of OPV and GNPs. The OPV solution was prepared by dissolving 4 mg in 10.00 mL DMF. Dissolving 4 mg GNPs in 10.00 mL DMF and shocking to prepare the GNPs solution. The total volume is 2.00 mL.

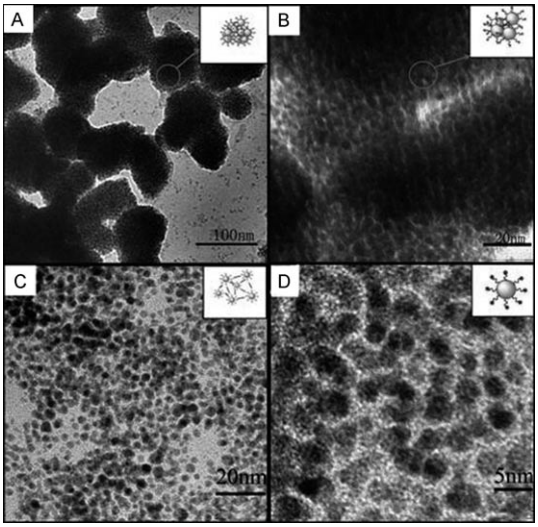

Figure 5. TEM images A) amino-terminated GNPs, B) HR–TEM of amino-terminated GNPs, C) the nanonetworks of GNPs–OPV, D) HR–TEM of GNPs–OPV.

GNPs, which generate the H-bonding leading to this aggregation. However, the reaction of amino with the epoxy groups at the terminals of OPV eliminate (or decrease) the effect of H-bonding. We can draw that conclusion easily from the image of Figure 5C, because the nanoparticles embedded in the nanonetworks do not lie in a plane but pile up. Consequently, the crystal lattices of the nanoparticles in HR–TEM (Figure 5D) appear discretely, which confirms the formation of nanonetworks.

We also adopt an analogous molecule (see Supporting Information) as a comparison to confirm the role of the as-prepared OPV in the construction of the nanonetworks. The analogous molecule bearing double hydroxyl groups looses the ability to react with amino functionalized GNPs, so it could not improve the dispersivity of the GNPs in the system. This indirectly proofs the ability of the as-prepared OPV in constructing the GNPs–OPV nanonetworks (Figure 6). The reaction occurs on the surfaces of the nanoparticles is critical to construct the novel organic–inorganic nanonetworks.

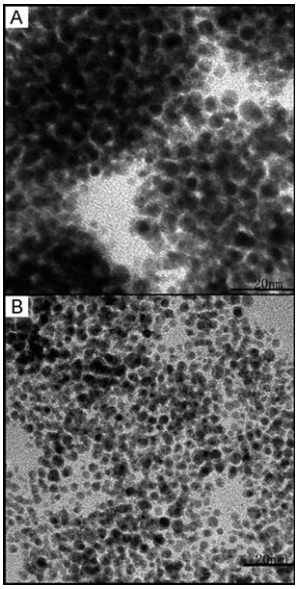

Figure 6. TEM images of the two molecules' role in the dispersivity of GNPs. A) the hydroxyl-terminated OPV and GNPs, B) the epoxide-terminated OPV and GNPS.

3. Conclusions

In summary, we have developed a novel strategy for the construction of nanonetworks of OPV and GNPs. The functionalization of nanoparticles with simple difunctional molecules serves as chemical reagents in the synthesis of nanohybrids. This illustrates that the GNPs could be further explored for nanoscale building blocks with modification by various simple ligands, extending to interdisciplinary applications. The resulting GNPs–OPV nanocomposites exhibit homogeneous and well-defined interfaces between the organic ligands and the inorganic nanoparticles, thereby promoting the efficient electronic interfacial interaction between the two constituents, facilitating the fabrication of fantastic devices. The methodology also provides a new application of amine reacting with epoxide beyond the traditional usage in discipline of macromolecules.

Experimental Section

Materials and methods: Chemicals were purchased from Alfa Aesar and Aldrich, and utilized as received unless indicated otherwise. All solvents were purified using standard procedures.

Synthesis and Characterization of 4-(oxiran-2-ylmethoxy)Benzaldehyde (1): 4-hydroxybenzaldehyde (1 g, 8.2 mmol) and potassium carbonate (3.4 g, 24.6 mmol) were suspended in 30 mL of ethanol and heated to 80 °C under nitrogen atmosphere. The mixture was vigorously stirred and the epoxy chloropropane (1.8 g, 19 mmol) was added dropwise within 10 min. After refluxing for 2 h, the resulting mixture was filtered to remove potassium carbonate and the filtrate was condensed on rotary evaporator. The residue was dissolved in ethyl acetate, washed with water, dried over anhydrous sodium sulfate, evaporated solvent. The resulting solid loaded on a silica column chromatography (eluent: petroleum ether : ethyl acetate = 5:1) to yield **1** (1.3 g, 89.3%) as white solid. ^{1}H NMR (400 MHz, $CDCl_3$, TMS) δ 2.79 (2H, J = 65.72 Hz), 3.39(1H, m), 4.35 (2H, J = 132 Hz), 7.04 (2H, J = 8.6 Hz), 7.85 (2H, J = 8.6 Hz). ^{13}C NMR(100 MHz, $CDCl_3$, TMS) δ 44.52, 49.85, 69.04, 114.92, 130.36, 131.98, 163.40, 190.75.

Synthesis of 1,4-Bis(dodecyloxy)benzene (2)[46]: To a suspension of 1,4-dihyroxyquinone (3.3 g, 10 mmol) and 1-bromododecane (5.3 g, 21 mmol) in 60 mL ethanol under nitrogen atmosphere, potassium hydroxyl (2.5 g, 45 mmol) was added all at once. After refluxing for 8 h, the reaction mixture was cooled to room temperature and filtered off, washed with ethanol and dried in vacuum. The crude product was recrystallized in methanol to yield **2** (4.1 g, 92.0%) as a white solid.

Synthesis of 1,4-Bis(bromomethyl)-2,5-bis(dodecyloxy)benzene (3)[46]: To a suspension of 1,4-bis(dodecyloxy)benzene (3.0 g, 6.7 mmol), paraformaldehyde (0.404 g, 13.4 mmol) and hydrogen bromide (2.00 mL, 45(wt)% in acetic acid, 13.4 mmol) was heated to 65 °C for 5 h. The resulting solution was cooled to room temperature and poured into 200 mL of water. The precipitate was filtered, washed by water and methanol. The product **3** (3.5 g, 83.0%) was obtained by recrystallizing from dichloromethane and methanol.

Synthesis of Tetraethyl(2,5-bis(dodecyloxy)-1,4-phenylene)bis-(methylene) diphosphonate (4): The mixture of 1,4-bis(bromomethyl)-2,5-bis(dodecyloxy)benzene (3.2 g, 5 mmol) and triethyl phosphate (1.66 g, 10 mmol) was heated to 140 °C for 8 h. The resulting solution was cooled to room temperature and loaded on silica gel chromatography (eluent: petroleum ether: ethyl acetate = 2:1) to give **4** (2.7 g, 72.2%) as a white solid.

Synthesis and Characterization of Oligo(phenylenevinylene) (5): To the solution of compound **1** (1 g, 5.6 mmol) and compound **4** (2.1 g, 2.8 mmol) dissolved in fresh THF (40 mL), sodium hydride (excess) was added slowly, and stirred for further 2 h. The excess sodium hydride was quenched by water when the reaction completed. The solvent was removed on rotary evaporator and washed by water (100 mL × 3) and brine, dried over Na_2SO_4. The residue was loaded on silica gel chromatography (eluent: petroleum ether:dichloromethane = 1:1) after evaporation of the solvent. The yellowish solid was obtained as OPV (**5**) (1.3 g, 59.5%) as light yellow powder. ^{1}H NMR (400 MHz, $CDCl_3$, TMS) δ 0.88 (6H, t), 1.50 (32H, m), 1.86 (4H, q), 2.85 (4H, q ,J = 59.40 Hz), 3.37(2H, m), 4.11 (4H, q, J = 97.84 Hz), 4.04 (4H, t), 6.92 (2H, d, J = 8.6 Hz),6.70–7.36 (6H, m),7.46 (4H,d, J = 8.6 Hz), ^{13}C NMR ($CDCl_3$, 400 MHz, TMS) δ 14.28, 22.84, 26.44, 25.52, 29.61, 29.66, 29.79, 29.81, 29.86, 32.07, 4.89, 50.27, 68.93, 69.73, 110.63, 114.94, 121.90, 126.94, 127.86, 128.14, 131.54, 151.09, 158.13. MS(TOF): 795.14(M).

Synthesis of Amino-Functionalizationed Gold Nanoparticles: The functionlized GNPs were prepared according to previous methods,[41,47] specifically, solution of 50 mg of $HAuCl_4{\cdot}4H_2O$ in 2.0 mL of deionized water and 300 mg of tert-n-octylammonium bromide in 5 mL of toluene were shaken in a separation funnel. The yellow water layer becomes clear and the $AuCl_4^-$ was phase transferred to organic layer. The organic layer was transferred to a 10 mL round-bottom bottle. Upon vigorously stirred, a freshly prepared solution of 5 mg of NaBH4 in 1 mL of deionized water was added all at once after which the solution darken. After 4 h of stirring the water was removed by extracted and the organic layer was washed several times. To the organic phase, 10 mg of 4-aminobenzenethiol (4-ATP) was added and the solution was stirred vigorously for 2 days. Subsequently, the toluene was evaporated and the black residue was suspended in ethanol and washed extensively over a glass frit with ethanol and acetone until the filtrate remained colorless. The trace of 4-aminobenzenethiol was monitored by TLC. The 4-ATP protected gold nanoparticles was obtained, which was dried for further usage.

Preparation of GNPs–OPV Networks: The OPV (1.5 mg) and previous prepared GNPs (1 mg) were mixed in 3 mL of *N*,*N*-dimethyl formamide (DMF) and then zinc perchlorate (Cat.) was added. The solution was stirred for 2 h and the amino added to epoxide under the catalysis of $Zn(ClO_4)_2{\cdot}6H_2O$.[39] The resulting solution was diluted and prepared as samples without further treatment to remove residual OPV.

Characterizations: TEM samples were prepared by dropping DMF solutions of GNPs on carbon coated copper grids (400 mesh) and evaporated. Images of representative areas were recorded on a JEOL JEM-2011 transmission electron microscope operating at 200 KV. The absorption spectra were obtained from DMF solutions of the gold nanoparticles on a JASCO V-570 spectrophotometer. The emission spectra were obtained on JASCO FP-6600 fluorimeter. Quartz cuvettes of 1 cm path length were employed. Proton and carbon nuclear magnetic resonance spectra (^{1}H NMR and ^{13}C NMR) were recorded out on Bruker ARX300, ARX400 spectrometer using tetramethylsilane (TMS) as an internal standard, chemical shifts are given in ppm relative to TMS. Mass spectra were measured with Bruker Biflex III MALDI-TOF spectrometer and APEX II FT-ICRMS spectrometer. The nanoparticles diameter distribution was recorded on Zetasizer.

Acknowledgements

This work was supported by the National Nature Science Foundation of China (20831160507,10874187,20873155 and 20721061) and the National Basic Research 973 Program of China.

Keywords: epoxides · gold nanoparticles · nanohybrids · nanonetworks · ring-opening reaction

[1] L. N. Lewis, *Chem. Rev.* **1993**, *93*, 2693 – 2730.
[2] J. Sharma, R. Chhabra, A. Cheng, J. Brownell, Y. Liu, H. Yan, *Science* **2009**, *323*, 112 – 116.
[3] P. V. Kamat, *J. Phys. Chem. B.* **2002**, *106*, 7729 – 7744.
[4] L. A. Dick, A. D. McFarland, C. L. Haynes, R. P. Van Duyne, *J. Phys. Chem. B.* **2002**, *106*, 853 – 860.
[5] M. C. Daniel, D. Astruc, *Chem. Rev.* **2004**, *104*, 293 – 346.
[6] K. J. Watson, J. Zhu, S. T. Nguyen, C. A. Mirkin, *J. Am. Chem. Soc.* **1999**, *121*, 462 – 463.

[7] R. L. Phillips, O. R. Miranda, D. E. Mortenson, C. Subramani, V. M. Rotello, *U. H. F. Bunz Soft Matter* **2009**, *5*, 607 – 612.
[8] R. L. Phillips, O. R. Miranda, C.-C. You, V. M. Rotello, U. H. F. Bunz, *Angew.-Chem.* **2008**, *120*, 2628; *Angew. Chem. Int. Ed.* **2008**, *47*, 2590 – 2594.
[9] N. A. K. Z. Tang, *Adv. Mater.* **2005**, *17*, 951 – 962.
[10] A. W. Tang, F. Teng, S. Xiong, Y. H. Gao, C. J. Liang, Y. B. Hou, *J.Photochem. Photobiol. A* **2007**, *192*, 1 – 7.
[11] R. Vendamme, S. Y. Onoue, A. Nakao, T. Kunitake, *Nature Mater.* **2006**, *5*, 494 – 501.
[12] S. H. Sun, D. Q. Yang, D. Villers, G. X. Zhang, E. Sacher, J. P. Dodelet, *Adv. Mater.* **2008**, *20*, 571 – 574.
[13] Y. Sun, Y. Xia, *Science* **2002**, *298*, 2176 – 2179.
[14] N. L. Rosi, D. A. Giljohann, C. S. Thaxton, A. K. R. Lytton-Jean, M. S. Han, C. A. Mirkin, *Science* **2006**, *312*, 1027 – 1030.
[15] M. Zayats, A. B. Kharitonov, S. P. Pogorelova, O. Lioubashevski, E. Katz, I. Willner, *J. Am. Chem. Soc.* **2003**, *125*, 16006 – 16014.
[16] L. J. Sherry, R. C. Jin, C. A. Mirkin, G. C. Schatz, R. P. Van Duyne, *Nano Lett.* **2006**, *6*, 2060 – 2065.
[17] K. Sugawa, T. Akiyama, H. Kawazumi, S. Yamada, *Langmuir* **2009**, *25*, 3887 – 3893.
[18] S. Nie, S. R. Emory, *Science* **1997**, *275*, 1102 – 1106.
[19] G. Li, X. Wang, J. Li, X. Zhao, F. Wang, *Tetrahedron* **2006**, *62*, 2576 – 2582.
[20] Y. Song, T. Huang, R. W. Murray, *J. Am. Chem. Soc.* **2003**, *125*, 11694 – 11701.
[21] H. Imahori, Y. Kashiwagi, Y. Endo, T. Hanada, Y. Nishimura, I. Yamazaki, Y. Araki, O. Ito, S. Fukuzumi, *Langmuir* **2004**, *20*, 73 – 81.
[22] E. Braun, Y. Eichen, U. Sivan, G. Ben-Yoseph, *Nature* **1998**, *391*, 775 – 778.
[23] S. Park, J. H. Lim, S. W. Chung, C. A. Mirkin, *Science* **2004**, *303*, 348 – 351.
[24] A. Ogawa, M. Maeda Bioorg, *Med. Chem. Lett.* **2008**, *18*, 6517 – 6520.
[25] W. Zhao, S. X. Sun, J. J. Xu, H. Y. Chen, X. J. Cao, X. H. Guan, *Anal. Chem.* **2008**, *80*, 3769 – 3776.
[26] K.-M. Sung, D. W. Mosley, B. R. Peelle, S. Zhang, J. M. Jacobson, *J. Am. Chem. Soc.* **2004**, *126*, 5064 – 5065.
[27] Zhiqun Lin, *Chem. Eur. J.* **2008**, *14*, 6294 – 6301.
[28] M. Brust, J. Fink, D. Bethell, D. Schiffrin, C. Kiely, *J. Chem. Soc., Chem. Commun.* **1995**, 1655 – 1656.
[29] T. G. Schaaff, G. Knight, M. N. Shafigullin, R. F. Borkman, R. L. Whetten , *J. Phys. Chem. B.* **1998**, *102*, 10643 – 10646.
[30] H. Z. Yu, J. Zhang, H. L. Zhang, Z. F. Liu, *Langmuir* **1999**, *15*, 16 – 19.
[31] X. F. Liu, X. R. He, T. G. Jiu, M. J. Yuan, J. L. Xu, J. Lv, H. B. Liu, Y. L. Li, *ChemPhysChem* **2007**, *8*, 906 – 912.
[32] P. Ionita, F. Spafiu, C. Ghica, *J. Mater.Sci.* **2008**, *43*, 6571 – 6574.
[33] I. Hussain, S. Graham, Z. Wang, B. Tan, D. C. Sherrington, S. P. Rannard, A. I. Cooper, M. Brust, *J. Am. Chem. Soc.* **2005**, *127*, 16398 – 16399.
[34] S. Abraham, I. Kim, C. A. Batt, *Angew. Chem.* **2007**, *119*, 5822 – 5825; *Angew. Chem. Int. Ed.* **2007**, *46*, 5720 – 5723.
[35] T. Skotheim, J. Reynolds, *Handbook of Conducting Polymers*, CRC, Boca Raton, **2007,** 14-1.
[36] E. W. L. Chan, D.-C. Lee, M.-K. Ng, G. Wu, K. Y. C. Lee, L. Yu, *J. Am. Chem. Soc.* **2002**, *124*, 12238 – 12243.
[37] H. Nakashima, K. Furukawa, K. Ajito, Y. Kashimura, K. Torimitsu, *Langmuir* **2005**, *21*, 511 – 515.
[38] R. Fernández, M. Miren Blanco, J. Galante, P. A. Oyanguren, M. Ianki, *J. Appl. Polym. Sci.* **2009**, *112*, 2999 – 3006.
[39] Shivani, B. Pujala, A. K. Chakraborti, *J. Org. Chem.* **2007**, *72*, 3713 – 3722.
[40] J. Boutagy, R. Thomas, *Chem. Rev.* **1974**, *74*, 87 – 99.
[41] M. Brust, M. Walker, D. Bethell, D. Schiffrin, R. Whyman, *J. Chem. Soc., Chem. Commun.* **1994**, 801 – 802.
[42] M. J. Hostetler, A. C. Templeton, R. W. Murray, *Langmuir* **1999**, *15*, 3782 – 3789.
[43] S. D. Evans, S. R. Johnson, H. Ringsdorf, L. M. Williams, H. Wolf, *Langmuir* **1998**, *14*, 6436 – 6440.
[44] E. R. Zubarev, J. Xu, A. Sayyad, J. D. Gibson, *J. Am. Chem. Soc.* **2006**, *128*, 4958 – 4959.
[45] J. Xu, J. Wang, M. Mitchell, P. Mukherjee, M. Jeffries-EL, J. W. Petrich, Z. Lin, *J. Am. Chem. Soc.* **2007**, *129*, 12828 – 12833.
[46] B. Wang, M. R. Wasielewski, *J. Am. Chem. Soc.* **1997**, *119*, 12 – 21.
[47] J. van Herrikhuyzen, R. A. J. Janssen, E. W. Meijer, S. C. J. Meskers, A. P. H. J. Schenning, *J. Am. Chem. Soc.* **2006**, *128*, 686 – 687.

Received: September 18, 2009
Published online on January 18, 2010

